Magnetic structure of zinc-substituted magnetite at $T = 4.2$ K

P. A. Dickof,* P. J. Schurer,† and A. H. Morrish
Department of Physics, University of Manitoba, Winnipeg, Manitoba R3T 2N2, Canada
(Received 19 December 1979)

The magnetic structure of $Zn_xFe_{3-x}O_4 (0 \leq x \leq 0.8)$ has been investigated by ^{57}Fe Mössbauer spectroscopy at $T = 4.2$ K. A localized canting model that considers the configurational details of the neighbors has been developed for the analyses of the spectral data. The magnetization predicted for the compounds with canted structures agrees reasonably well with the values determined by experiment.

I. INTRODUCTION

Mixed Zn ferrites of the type $Zn_xM_{3-x}O_4$ where M is a magnetic ion have been the subject of numerous investigations in the past, especially with regard to their magnetic properties.[1] The metallic ions occupy the tetrahedral A or octahedral B sites in the spinel crystal structure. The Zn ions preferentially occupy the A sites because of their tendency to form covalent bonds involving sp^3 orbitals. For $x = 0$, the magnetic moments on the more numerous B sites lie along the magnetization direction; those on the A sites are aligned antiparallel. Therefore, the substitution of diamagnetic Zn^{2+} ions for the M ions on the A sublattice may reasonably be expected to result in an increase in the magnetization, proportional to the amount of substitution, at $T = 0$ K. Such indeed occurs for $x \lesssim 0.5$, although the increase is less than expected if free-ion magnetic moments for the M ions are assumed. At higher Zn concentrations, i.e., $x \gtrsim 0.5$, the moment begins to decrease and for $x = 1.0$, an antiferromagnetic structure is observed.[2] Although several other models[3–5] have been offered for the behavior of the magnetization for $x \gtrsim 0.5$, spin canting has been determined to be primarily responsible. The canting angles have been measured for several systems using the neutron diffraction[6,7] or the Mössbauer technique.[8–15] From the measured values of the canting angles it is possible in principle to fit the magnetization results quantitatively. No such work has yet been reported. Magnetization and Mössbauer results have usually been determined for different samples, and at differing temperatures and fields. A quantitative determination of the canting angles should allow a decision to be made on whether or not the spin canting is solely responsible for the magnetization behavior. However a ^{57}Fe Mössbauer study can only give information about canting of the iron magnetic moments. Therefore, the only mixed Zn spinel for which a complete correlation between magnetization and ^{57}Fe Mössbauer measurements is possible is the $[Zn_x^{2+}Fe_{1-x}^{3+}](Fe_{1-x}^{2+}Fe_{1+x}^{3+})O_4$ family. Here the square and round brackets indicate cations on the A and B site, respectively. This system was first studied by Stuijts *et al.*[16] at 4.2 K for $x \leq 0.7$ and most recently by Srivastava *et al.*[17,18] between 77 and 300 K for $x \leq 0.8$. As with other mixed Zn ferrites, the magnetization was shown to increase with increasing x until $x \simeq 0.5$, after which it began to decrease.

The main purpose of the present study is to compare quantitatively the magnetization values measured at 4.2 K with those calculated from the microscopic spin structure as determined from a ^{57}Fe Mössbauer investigation.

II. THEORY

The exchange interactions for the A and B sublattices of the spinel structure of a ferrite can be represented by three exchange parameters: J_{AB}, the intersublattice exchange parameter and J_{AA} and J_{BB}, the intrasublattice exchange parameters. If only nearest-neighbor superexchange bonds are considered then the local mean field for a spin on the ith sublattice can be written, following the notation of Rosencwaig,[19] as:

$$\vec{H}_i = (2/g\mu_B)(J_{ij}\vec{S}_j + J_{ii}\vec{S}_i) \quad , \tag{1}$$

where $\vec{S}_i$ and $\vec{S}_j$ represent the sum of the neighboring spins on either sublattice. For example, the B sublattice of $[Fe^{3+}](Fe^{2+}Fe^{3+})O_4$ has

$$|\vec{S}_A| = 6\mu_\alpha/g\mu_B, \quad |\vec{S}_B| = 6\mu_\beta/g\mu_B \quad .$$

Here μ_α and μ_β are the magnetic moments per atom of spins on the A and B sublattices, respectively. As J_{AB} is much more negative than J_{AA} and J_{BB} the two sublattices are arranged in an antiparallel fashion as shown in Fig. 1(a).

In $[Zn_x^{2+}Fe_{1-x}^{3+}](Fe_{1-x}^{2+}Fe_{1+x}^{3+})O_4$, diamagnetic Zn^{2+} ions are randomly substituted into the A sublattice, resulting in a change in $\vec{S}_A$ and $\vec{S}_B$, and in a breaking of nearest-neighbor exchange interactions. Geller *et al.*[20] proposed that random canting occurred on the *unsubstituted* lattice under these conditions on the

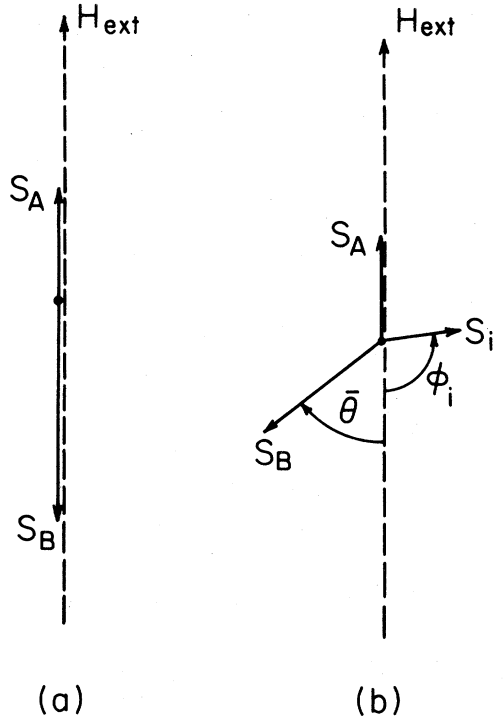

FIG. 1. Schematic representation (a) of a collinear spin structure and (b) of a canted spin structure. The average canting angle on the B sublattice is indicated by $\bar{\theta}$ and the local canting angle by ϕ_i.

basis of their experimental data. This proposal was developed mathematically by Rosencwaig[19] for the yttrium iron garnet (YIG) system and is outlined here for spinels.

A random distribution of diamagnetic ions is assumed on the A sublattice and canting angles ϕ with respect to the magnetization axis are assumed on the B sublattice. This allows us to write the local mean field for a given ion i on the B sublattice by using Eq. (1). However, since there is diamagnetic substitution on the A sublattice,

$$|\vec{S}_A| = (6-m)\mu_\alpha / g\mu_B \ , \tag{2a}$$

where m is the number of neighboring sites on the A sublattice which are occupied by diamagnetic ions. Similarly, for the B sublattice

$$|\vec{S}_B| = 6\mu_\beta(x)/g\mu_B \ , \tag{2b}$$

where $\mu_\beta(x) = (1-x)\mu_\beta^{2+} + (1+x)\mu_\beta^{3+}$ and μ_β^{2+} and μ_β^{3+} represent the ionic moments of the B site Fe^{2+} and Fe^{3+} ions, respectively. This relationship for $\mu_\beta(x)$ assumes complete d-electron localization, which is reasonable even for magnetite below the Verwey temperature.

The resultant spin structure, with the spin S_i taking a local canting angle ϕ_i with respect to the magnetization direction is shown in Fig. 1(b). Here the A sublattice is represented by a single spin of magnitude $|\vec{S}_A|$ [Eq. (2a)] aligned opposite the magnetization direction, and the B sublattice is represented by a single spin of magnitude $|\vec{S}_B|$ [Eq. (2b)] at a canting angle $\bar{\theta}$, the average canting angle of the B sublattice with respect to the magnetization direction. It follows from this assumption, Eq. (1), and negligibly small J_{AA}/J_{AB} that the local canting angle $\phi_i(m)$ is given by

$$\cos[\phi_i(m)] = \frac{|\vec{S}_A| - |\vec{S}_B|\delta\cos\bar{\theta}}{[|\vec{S}_A|^2 + (|\vec{S}_B|\delta)^2 - 2|\vec{S}_A||\vec{S}_B|\delta\cos\bar{\theta}]^{1/2}}$$

where $\delta = J_{BB}/J_{AB}$.

It follows that $\phi_i(m)$ can take on any value between 0° and $(180° - \bar{\theta})$ depending on the value of the numerator. If $S_A > S_B\delta\cos\bar{\theta}$, i.e., if the net intersublattice interaction on a spin is greater than the net intrasublattice interaction, then $\phi_i(m)$ will be smaller than the average canting angle $\bar{\theta}$. If $S_A < S_B\delta\cos\bar{\theta}$, then $\phi_i(m)$ will be larger than the average canting angle $\bar{\theta}$, and if $S_A = 0$, then the B_i spin will be aligned antiparallel to S_B, that is, with a canting angle $\phi_i = -\bar{\theta}$. The result of this analysis is therefore that the local canting angle of the B-site ion depends (via S_A) on the number of diamagnetic nearest neighbors on the A sites and on the ratio J_{BB}/J_{AB}. If a random distribution is assumed, the probability of a spin having m of its six A-site neighbors occupied by Zn^{2+} ions can be calculated from the binomial distribution:

$$P(x,m) = \binom{6}{m} x^{6-m}(1-x)^m \ ,$$

which allows the magnetic moment per formula unit to be written

$$\mu(x,T=0) = 2\sum_{m=0}^{6} P(x,m)\cos[\phi(x,m)]\mu_\beta(x) - (1-x)\mu_\alpha \ . \tag{3}$$

The first term indicates the decrease in moment due to random canting on the B sublattice, and the second represents the increase in moment due to diamagnetic substitution on the antiparallel A sublattice.

The model developed by Rosencwaig has been used successfully in the past for a qualitative description of canting in several mixed Zn ferrites. Before applying the model in a quantitative fashion however, it is necessary to make some modifications. In the first place, it should be noted that the representation of the neighboring B-sublattice spins $\vec{S}_j$ and their canting angles ϕ_j by $|\vec{S}_B|$ and the average B-sublattice canting angle $\bar{\theta}$ is not very good. A better representation is given by a vector summation of the B-sublattice nearest-neighbor spins. Thus Eq. (2b) is

replaced by

$$\vec{S}_B = \left[\sum_{j=1}^{6} S_j \cos(\phi_j)\cos(\psi_j)\right]\hat{x} + \left[\sum_{j=1}^{6} S_j \cos(\phi_j)\sin(\psi_j)\right]\hat{y} + \left[\sum_{j=1}^{6} S_j \sin(\phi_j)\right]\hat{z} \ , \tag{4}$$

where the ψ_j are the azimuthal angles of the spin. Now, using Eq. (1) as before, it follows that:

$$\cos[\phi_i(m_i)] = \frac{|\vec{S}_A(m_i)| - |\vec{S}_B|\delta\cos[\alpha_i(m_i)]}{\{|\vec{S}_A(m_i)|^2 + |\vec{S}_B|^2\delta^2 - 2|\vec{S}_A(m_i)||\vec{S}_B|\delta\cos[\alpha_i(m_i)]\}^{1/2}} \ , \tag{5}$$

where $\alpha_i(m_i)$ is the angle that the resultant $\vec{S}_B$ [of Eq. (4)] makes with the magnetization axis. This angle will, in general, be very different from $\bar{\theta}$, the average canting angle of the B sublattice, and will be smaller than $\sum_{j=1}^{6} \frac{1}{6}\phi_j$ because the spins will be randomly distributed over the azimuthal angle ψ_j. In practice, it will be very difficult to calculate $\alpha_i(m_i)$ and thus, to determine δ from Eq. (5).

The second modification required for the localized canting model occurs because nearest B-sublattice neighbors share some of the same A sites as nearest A-sublattice neighbors. Thus the surroundings of neighboring B-sublattice ions are not independent of each other. Once we choose a spin $\vec{S}_i$ having m_i zinc A-sublattice nearest neighbors, the probabilities for the possible values of m_j and ϕ_j available to each of the nearest B-site neighbor spins $\vec{S}_j$ are no longer given by the binomial distribution. This means that α_i is a function of m_i as we have already implied in Eq. (5). When $\phi_i(m_i) > 90°$, such spins being referred to as reversed spins, this m_i dependence of α_i affects the orientation of $\vec{S}_i$ in a very dramatic way.

Since, in the ferrites $|J_{AB}|$ is known to be much larger than $|J_{BB}|$, we will assume that only those spins with all six nearest A-sublattice neighbors occupied by Zn ions can be reversed. If more than half of the nearest B-sublattice neighbors of one of these reversed spins are themselves reversed, then that spin will have been reversed twice. Similarly, if the neighbors to a reversed spin are themselves doubly reversed, that spin will have been triply reversed. It is thus clear that any theory which considers *only* first-nearest neighbors will break down if multiple-reversal probabilities become significant. The probabilities for multiple reversal to occur can be calculated by assuming a random distribution of Zn^{2+} ions on the A sublattice and considering the number of spins shared by all the neighbors. The multiple reversal probabilities are very small for $x \leq 0.4$; i.e., the first order of reversal gives a satisfactory picture. For $x = 0.6$ and 0.8, calculations must be made to second and third order, respectively, the results of which are shown in Table I.[21] This allows determination of the total number of magnetic moments reversed or unreversed with respect to the magnetization direction as given in Table II. An attempt was made to perform a similar calculation for $x = 0.9$, but it was estimated that 4–6 orders of reversal would be required to give a satisfactory picture and it is extremely difficult to calculate that many orders. For $x = 0.95$, even more orders, perhaps 10–20 would be required.

The magnetic moment per formula unit at $T = 0$ K may now be written

$$\mu(x, T=0) = 2\left[\sum_{m=0}^{5} P(m,x)\cos[\phi(m,x)] + P(6'x)\cos[\phi(6',x)] + P(6,x)\cos[\phi(6,x)]\right]\mu_\beta - (1-x)\mu_\alpha \ , \tag{6}$$

where $m = 6$ refer to unreversed (or doubly reversed) spins at $m = 6'$ are the sum of singly and triply reversed spins (Table II). This modified localized canting model will be used for the analysis of the Mössbauer spectra and magnetization data presented in Secs. III–V.

TABLE I. Multiple-reversal probabilities for $Zn_xFe_{3-x}O_4$ where $x = 0.6$ and 0.8.

Sample x	Unreversed $(B_0 - B_5)$	Single reversal	Double reversal	Triple reversal
0.6	0.953 34	0.042 74	0.003 92	. . .
0.8	0.737 86	0.152 19	0.081 21	0.028 74

TABLE II. Probabilities for reversed and unreversed spins in $Zn_xFe_{3-x}O_4$ samples with $x = 0.6$ and 0.8.

Sample x	Unreversed (B_{05})	Reversed $(B_{6'})$	Unreversed (B_6)
0.6	0.953 34	0.042 74	0.003 92
0.8	0.737 86	0.180 93	0.081 21

III. EXPERIMENTAL

The samples were prepared by Srivastava *et al.*[17,18] in a way similar to that of Stuijts *et al.*[16] X-ray-diffraction techniques showed the samples to be free of impurity phases. The lattice parameters were measured and are plotted as a function of Zn concentration in Fig. 2. The linear increase in lattice parameter with Zn concentration derives from the large size of the Zn^{2+} ions as compared to the Fe^{3+} ions. The high-angle lines were not broadened, indicating that the samples had a uniform Zn distribution.

The magnetization measurements were performed using a vibrating-sample magnetometer, usually within the field of a regulated, water-cooled electromagnet. For fields in excess of 18 kOe, a superconducting solenoid was used for which a set of sensing coils was developed. The system was calibrated using a sphere of spectroscopically pure nickel and the values of Crangle and Goodman.[22]

The Mössbauer measurements were made with a constant-acceleration spectrometer which was calibrated by using iron-foil and α-Fe_2O_3 absorbers.[23] A linewidth of 0.28 mm/s is measured for the outer lines of an iron-calibration absorber 10 mg/cm^2 thick. The differential linearity[24] of the spectrometer is 0.2%. The isomer-shift values quoted in Sec. III are with respect to iron.

The external magnetic field produced by the superconducting solenoid has a negligible field decay during the time required to collect a Mössbauer spectrum. Magnetic shielding was used to reduce stray fields to below 100 Oe at the source, which was at room temperature during the measurement. The thickness of the absorbers was ~0.4 mg/cm^2 ^{57}Fe.

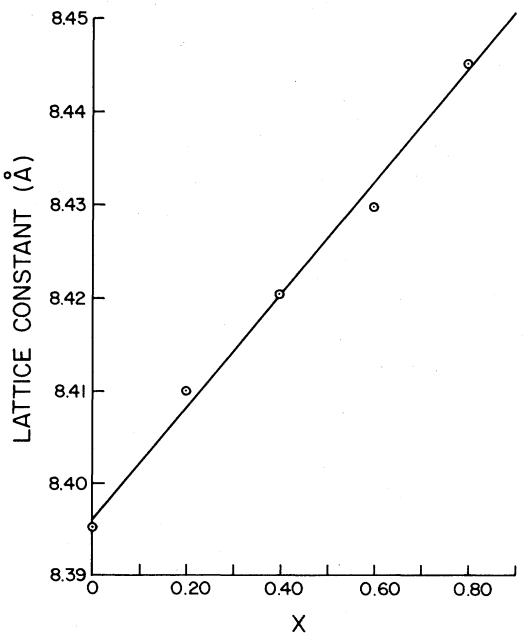

FIG. 2. Lattice parameter of $Zn_xFe_{3-x}O_4$ as a function of the Zn concentration x.

The Mössbauer spectra were fitted with one or more patterns consisting of Lorentzian absorption lines. All patterns were symmetrically constrained; i.e., the linewidth and depth of the first peak equals the linewidth and depth of the sixth peak, etc. The splitting ratios for the 2,5 lines as compared to the 1–6 lines were constrained to theoretical values.[23] This is necessary in view of the frequently small intensities of the 2–5 lines.

Since the sample was powdered and randomly oriented, the electric-field-gradient tensor was randomly orientated with respect to the applied magnetic axis throughout the sample. Therefore the quadrupole splitting was constrained to be zero; as expected some slight-line broadening was observed.

Canting angles were calculated for the various component spectra in order that the values could be used for the calculation of the bulk magnetization. Two methods can be used to calculate these angles: the intensity method, and the hyperfine-field method. The intensity method uses the ratios of the areas $A_{2,5}$ and $A_{1,6}$ of the 2–5 and 1–6 lines, respectively, of the various spectra and the formula

$$\phi = \arcsin\left[\frac{\frac{3}{2}(A_{2,5}/A_{1,6})}{1+\frac{3}{4}(A_{2,5}/A_{1,6})}\right]^{1/2},$$

where ϕ is the angle between the hyperfine field at the nucleus, and the direction (positive or negative) of the absorbed γ ray (here parallel to the applied magnetic field). This method is reasonably accurate ($\pm 10°$ or less) because the line intensities are usually well defined. For small angles ($\phi < 20°$) the relative error becomes large, but this has little effect on the calculated moments for the samples since $\cos\phi \approx 1$ in Eq. (6).

The hyperfine-field method for calculating the canting angles employs the cosine rule to solve for the canting angles (Fig. 3) and gives

$$\phi = \arccos\frac{H_{hf}^2(H_{ext}) - H_{hf}^2(0) - H_{ext}^2}{2H_{hf}(0)H_{ext}},$$

where $H_{hf}(H_{ext})$ is the hyperfine field in the presence of the applied field H_{ext}, and $H_{hf}(0)$ is the hyperfine field for $H_{ext}=0$. This method has some associated problems. The hyperfine fields, $H_{hf}(0)$ and $H_{hf}(H_{ext})$, can differ by at most H_{ext}. Further, if H_{ext} is small (~10 or 20 kOe), the hyperfine fields for a spectrum are not well resolved, and the errors in $H_{hf}(H_{ext})$ are an appreciable percentage, even up to 100%, of H_{ext} itself. It follows that the uncertainty in the numerator can lead to a very large error in the canting angle ϕ. Finally, experiments above 4.2 K,

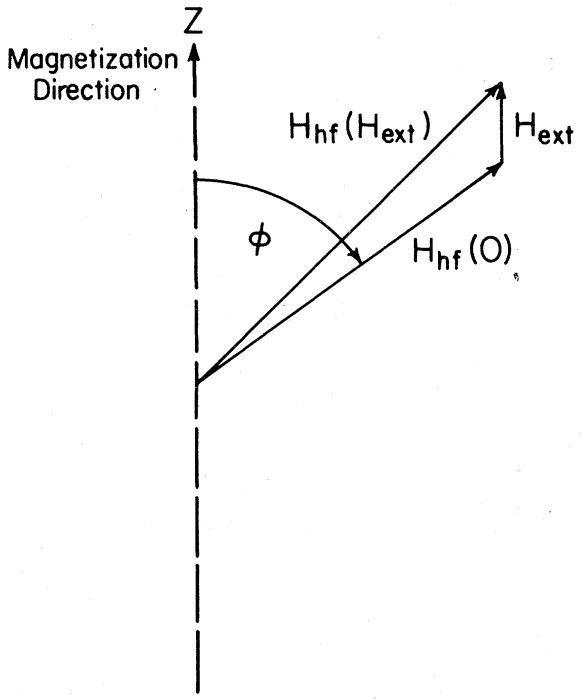

FIG. 3. Hyperfine fields with and without an external field, H_{ext}, applied and the canting angle.

and on which a future report is planned, indicate the $H_{hf}(H_{ext})$ changes in magnitude and orientation with H_{ext} in a manner that makes the hyperfine-field method no longer applicable. In view of these problems, only the canting angles, ϕ, calculated from the intensity method are presented in Sec. IV.

IV. EXPERIMENTAL RESULTS

A. Magnetization measurements

The values of the magnetization for the various samples are shown as a function of field at 4.2 K in Fig. 4. The results clearly show that the magnetization values increase for $x \leq 0.5$ and subsequently decrease for larger values of x. Figure 4 shows that the high-field susceptibilities of the various samples are quite different. For the samples with $x = 0.0$ and 0.2 saturation occurs in a field of approximately 8 kOe. Above 10 kOe, these samples have, within the experimental error, the same susceptibility with a value less than 0.05 emu/g/kOe. The samples with $x = 0.4$, 0.6, and 0.8, however, are clearly not saturated; they have average susceptibilities between 10 and 50 kOe of 0.19, 0.38, and 0.59 emu/g/kOe, respectively. At 50 kOe the susceptibilities are 0.08, 0.33, and 0.57 emu/g/kOe which indicates that for the $x = 0.4$ sample the canting is then very small. This behavior may be the result of a field dependence of the canting angles. For this reason we have determined the canting angles for various values of H_{ext}.

B. Mössbauer measurements

In zero applied magnetic field only the components corresponding to Fe^{2+} and Fe^{3+} ions are resolved. The linewidth of the Fe^{3+} component is $\sim$0.6 mm/s independent of zinc content, and does not permit the A- and B-site Fe^{3+} components to be resolved. Furthermore, it follows that the Fe^{3+} hyperfine field is not much affected by the distribution of neighboring Zn^{2+} ions. The Fe^{2+} component has a linewidth of $\sim$1.0 mm/s indicating a broader hyperfine-field distribution.

The hyperfine fields corresponding to spin components parallel and antiparallel to an applied magnetic field are resolved for $H_{ext} \gtrsim 30$ kOe. The attempts to analyze the Mössbauer spectra have been based mainly on the results for the fitting of these resolved spectra. Several models were used: the localized canting model with no reversed spins, the localized canting model with reversed spins developed by Rosencwaig,[19] and the modified localized canting model with multiple reversed spins discussed in Sec. II. As an example, the analyses of the $x = 0.8$ sample will be discussed.

The 4.2-K, 50-kOe spectrum (Fig. 5) was fitted first assuming that line a corresponds to A-site ions and line b to B-site ions. Line c was assumed to be due to canting on the B site alone. This yielded an A to B area ratio of 0.30:1, a value much higher than the ratio of 0.10:1 expected on the basis of the chemical formula. In addition, the calculated magnetization, assuming $\mu^{2+} = 4\mu_B$, $\mu^{3+} = 5\mu_B$, and using the canting angle obtained from Eq. (7) yields a magnetic moment of $7.2 \pm 0.2\mu_B$ per formula unit, a value 60% higher than the measured value of $4.47 \pm 0.04\mu_B$ per formula unit. The possibility that the anomalous A to B area ratio indicated the presence of Zn atoms on the B sites could be eliminated because at 20 and 40 K in fields of 50 kOe the spectra had an area ratio of 0.09 ± 0.01. Apparently at or above 20 K, only A-site ions contribute to the absorption of peak a, but at 4.2 K, the reversed B-site spins also contribute to the absorption of peak a. Also the Mössbauer spectra at 20 and 40 K established that with increasing temperature, peak b broadened, as expected, but that peak a narrowed. This latter observation also suggests the presence of more than one component in peak a at 4.2 K.

Reversal behavior is to be expected for those B sites with large numbers of Zn nearest neighbors according to the localized canting model. We next assumed that all B-site spins with six Zn nearest neighbors, denoted by $B_{6'}$, were reversed (that is $\phi > 90°$) and contributing to the areas of both peak a and peak

c. The structure visible in peak c helped to fit a pattern for the $B_{6'}$ ions. The ratio $(A+B_6)/B_{05}=0.35$ was obtained where the symbols now refer to areas and B_{05} is associated with the ensemble of iron ions on B sites with zero to five Zn nearest A-site neighbors. The theoretical ratio is 0.49 and still disagrees with experiment. In addition, the magnetization calculated with this model was $2.7 \pm 0.2 \mu_B$ per formula unit, a value 40% too low.

However, by making allowance for multiple reversals, a theoretical ratio $(A+B_{6'})/(B_{05}+B_6)=0.36$ was calculated, in excellent agreement with the ex-

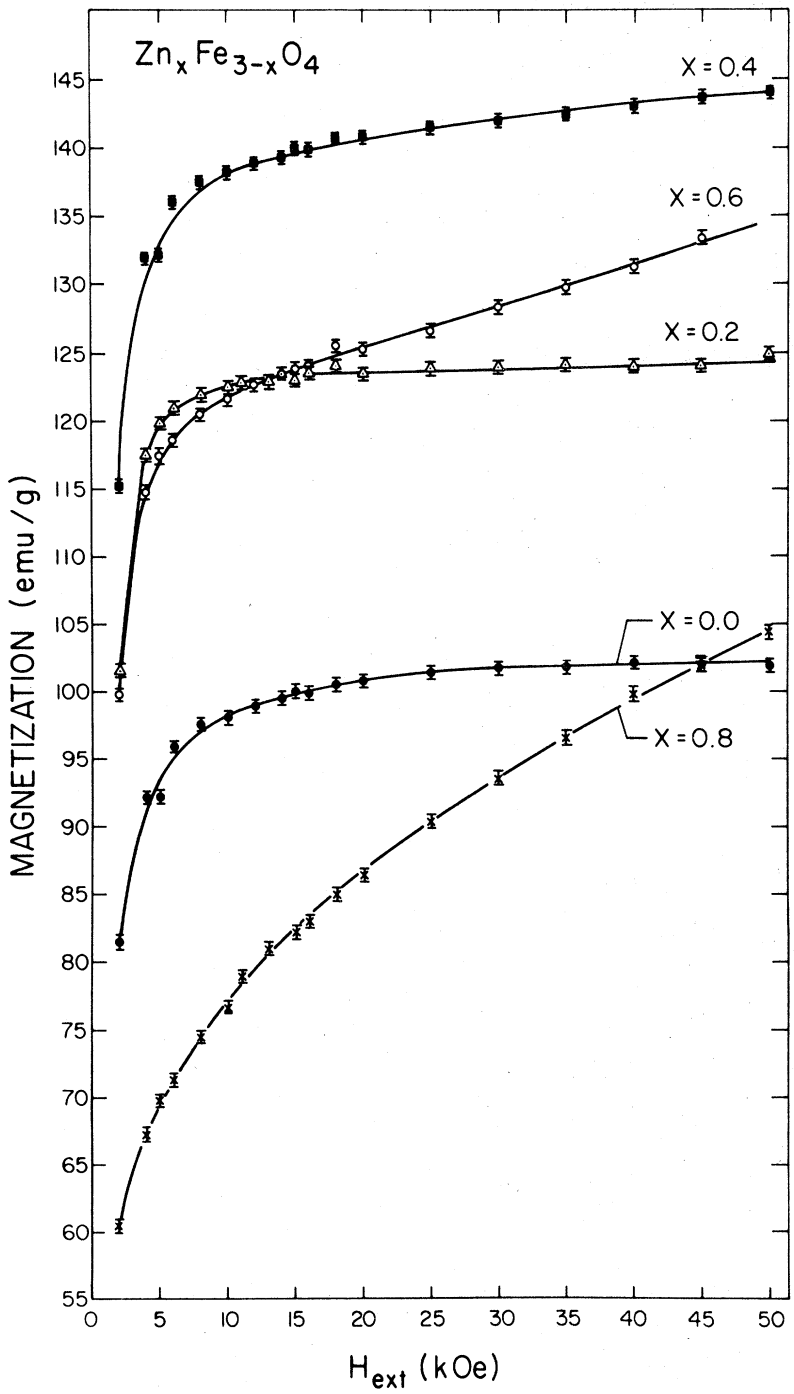

FIG. 4. Magnetization vs applied field for $Zn_xFe_{3-x}O_4$ at 4.2 K. The points with error bars represent the experimental data; the curves are drawn to fit these data.

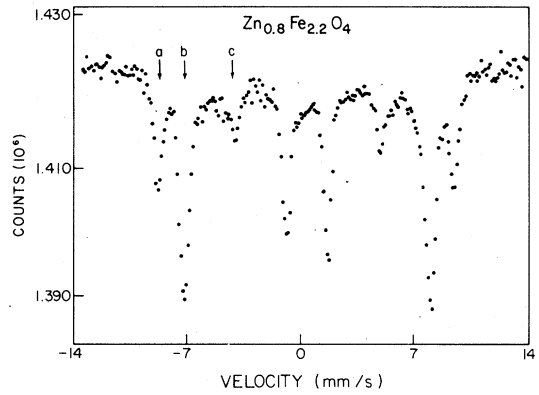

FIG. 5. Mössbauer spectrum of $Zn_{0.8}Fe_{2.2}O_4$ at 4.2 K and 50 kOe.

perimental value of 0.35. Here $B_{6'}$ refers to singly and triply reversed spins and B_6 to doubly reversed ones on B sites (see Fig. 6). Further, the magnetization then is calculated to be $4.2 \pm 0.2\mu_B$ per formula unit, a difference of 6% from the measured value. Clearly, the multiple reversal model gives the best

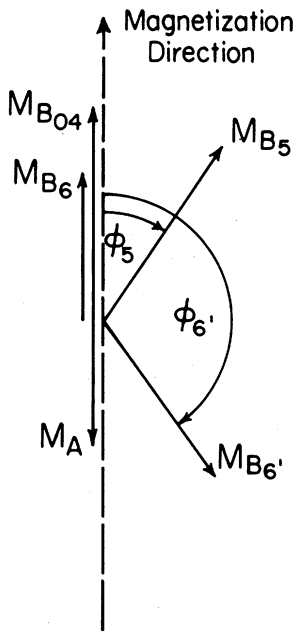

FIG. 6. Magnetic structure of $Zn_xFe_{3-x}O_4$ for $x = 0.6$ and 0.8.

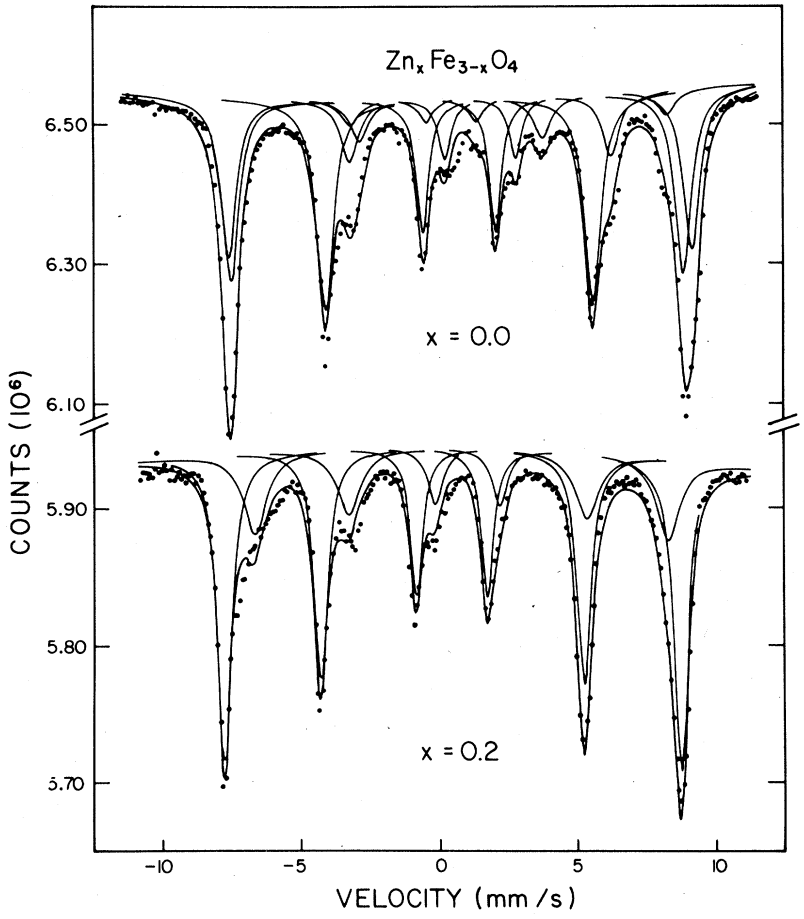

FIG. 7. Mössbauer spectra of $Zn_xFe_{3-x}O_4$ for $x = 0.0$ and 0.2 at 4.2 K and 0 kOe.

TABLE III. Experimental values of the isomer shift δ (mm/s), quadrupole shift ϵ' (mm/s), and hyperfine field H_{hf} (kOe) for Fe^{2+} ions in $Zn_xFe_{3-x}O_4$ for $H_{ext}=0$ kOe at 4.2 K. The subscripts I and II indicate the two patterns for ferrous ions fitted to magnetite. The figures in parentheses are the probable errors.

	Fe_I^{2+}			Fe_{II}^{2+}		
x	δ	ϵ'	H_{hf}	δ	ϵ'	H_{hf}
0.0	1.16(5)	−1.70(5)	508(1)	1.56(5)	2.07(5)	356(1)
0.2	0.89(4)	−0.50(4)	464(1)			
0.4	0.93(7)	−0.77(7)	450(1)			
0.6	0.92(5)	−0.54(5)	448(2)			
0.8			429(4)			

agreement between the Mössbauer and the magnetization data.

The Mössbauer spectra were fitted with an appropriate number of six-line patterns. When the resolution was sufficient, the errors were taken to be those given by the fitting program. When the patterns were not resolved, a larger error of 5 kOe in the hyperfine field was assigned in view of the uncertainty. When several components were treated as one six-line pattern, the error in the average hyperfine field was raised to 10 kOe. These two figures represent approximately one-quarter and one-half the linewidths of the fitted lines, respectively.

Below the Verwey temperature T_V, Fe_3O_4 exists in a multiple twinned monoclinic state.[25] As a result the lines in the Mössbauer spectrum are broadened because of the distribution of angles between the magnetic and the electric field gradient. The broadening can be removed by cooling a single-crystal specimen through T_V in a magnetic field applied along [100].[26] The spectrum obtained from such a specimen can be resolved into five components corresponding to one *A*-site Fe^{3+} ion, two *B*-site Fe^{3+} ions, and two *B*-site Fe^{2+} ions.[25,26] Rubinstein and Forester[27] have proposed six components corresponding to three Fe^{3+} sites and three Fe^{2+} sites.

Since the present Fe_3O_4 sample is polycrystalline and it is not the purpose of this investigation to discuss the properties of Fe_3O_4, the spectrum for Fe_3O_4 has been fitted with only one Fe^{3+} component and two Fe^{2+} components. The results are in fair agreement with those published previously in the literature.[25,26] For the $x=0.2$ sample only two components were fitted because the Fe^{2+} component with the smallest H_{hf} value is not present anymore. The data and computer fits are shown in Fig. 7. The associated Mössbauer parameters are listed in Table III for ferrous ions and in Table IV for ferric ions. Here the numbers in brackets are the errors in the last significant digit or digits.

No measurements in applied fields were performed for the $x=0.0$ and 0.2 samples. Previous studies

TABLE IV. Experimental values of the isomer shift δ (mm/s), hyperfine field H_{hf} (kOe), and average canting angle $\bar{\theta}$ (degrees) for Fe^{3+} ions in $Zn_xFe_{3-x}O_4$ at 4.2 K; the quadrupole shift $\epsilon=0.0(1)$ mm/s.

		A site		*B* site		
x	H_{ext}(kOe)	δ	H_{hf}	δ	H_{hf}	$\bar{\theta}$
0.0	0	0.82(1)	520(5)	0.82(1)	520(5)	
0.2	0	0.45(1)	511(5)	0.45(1)	511(5)	
0.4	0	0.45(1)	511(5)	0.45(1)	511(5)	
0.4	10	0.47(2)	511(5)	0.47(2)	511(5)	21(2)
0.4	50	0.39(1)	562(1)	0.50(2)	471(1)	<10

have already shown that for Fe_3O_4 the spin structure is collinear.[27] The susceptibility for the $x=0.2$ sample above 10 kOe is not significantly different from that of Fe_3O_4 (Fig. 4). By taking into account the experimental errors and assuming that any possible high-field susceptibility is the result of decreasing canting angles in an increasing magnetic field, an upper limit of 2° canting at 10 kOe can be estimated. Canting angles of such a small size ($<10°$) are difficult to measure.

For the $x=0.4$ sample, the $B_{6'}$ pattern is small and has been neglected. Also, the 2 and 5 lines for the Fe^{2+} pattern are difficult to resolve from those for the Fe^{3+} ions. Indeed, the error in the Fe^{2+} 2 and 5 line areas is about 70%; consequently no canting angles for the Fe^{2+} ions has been determined. Spectra in 0, 10, and 50 kOe applied fields, together with the computer fits, are shown in Fig. 8. In addition, the parameters deduced are tabulated in Tables III and IV.

For the $x=0.6$ and 0.8 samples with $H_{ext} \gtrsim 30$ kOe, the A and $B_{6'}$ components are separated from the B_{05} component. However, the A and $B_{6'}$ components are not resolved from each other. Therefore

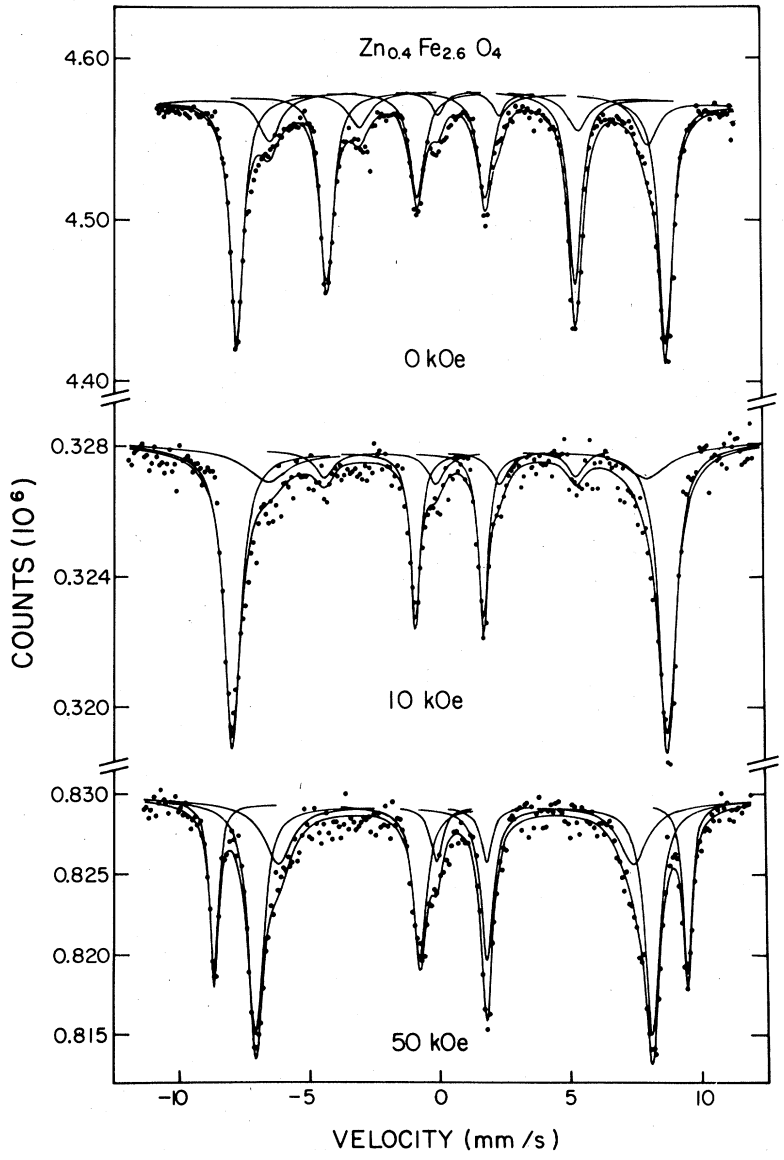

FIG. 8. Mössbauer spectra of $Zn_{0.4}Fe_{2.6}O_4$ at 4.2 K in applied fields of 0, 10, and 50 kOe.

they have been fitted separately by making use of the probabilities in Table II. Because the contribution the Fe^{2+} ions make to the absorption is relatively small, the canting of these ions has been assumed to be the same as that for Fe^{3+} ions. However, a separate B_5 component has been fitted. The B_0 to B_4 components have been combined into one component, B_{04} (see Fig. 6). The double reversed component, B_6, was fitted for $x = 0.8$, but was neglected for $x = 0.6$ (see Table II). The data and fits are shown in Figs. 9 and 10, and the parameters deduced are listed in Tables III and V.

The relatively few $B_{6'}$ spins are expected to align themselves antiparallel to the *average* B-site spin direction. The average canting angle for $x = 0.6$ in 50 kOe is close to 0° (see Fig. 9), and for smaller values of H_{ext} not much larger. Therefore, the $B_{6'}$ canting angle was taken as 180° for this composition. For $x = 0.8$, the canting angles at 30 and 50 kOe were 140° and 142°, respectively. Since these values seem to be field independent, the same canting angles were assigned for lower applied fields.

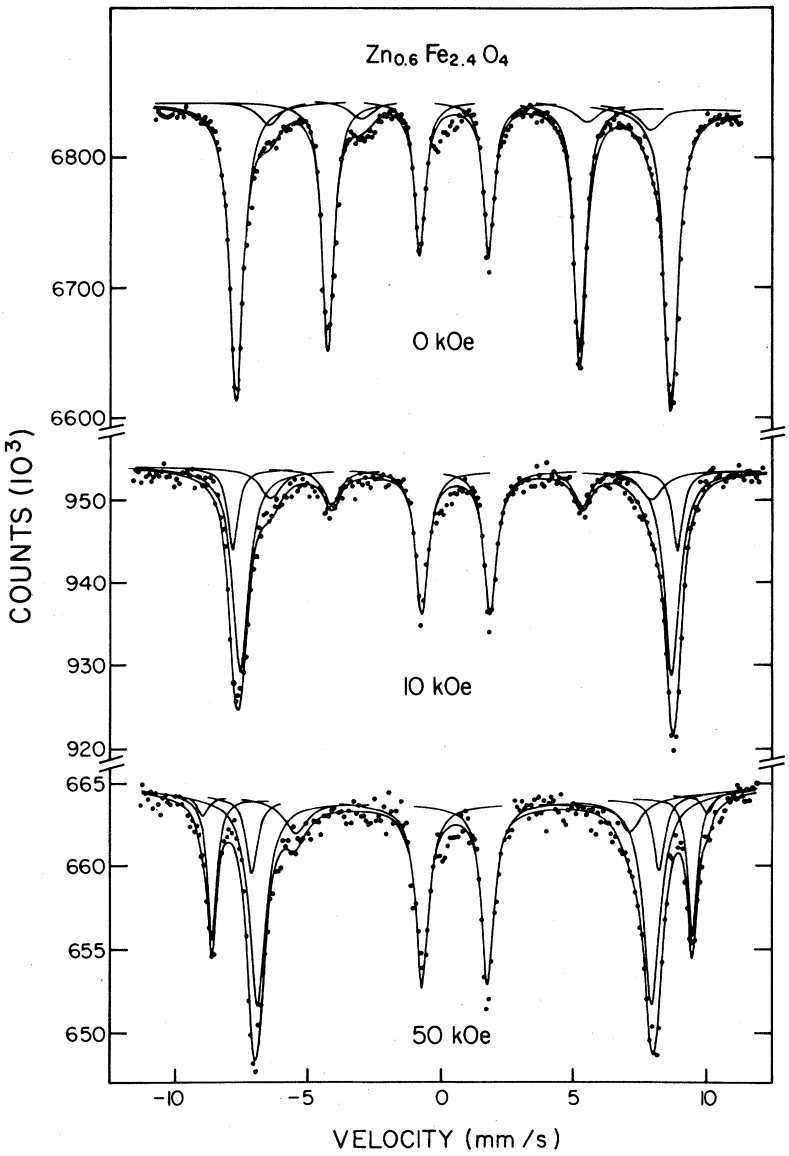

FIG. 9. Mössbauer spectra of $Zn_{0.6}Fe_{2.4}O_4$ at 4.2 K in applied fields of 0, 10, 25, and 50 kOe.

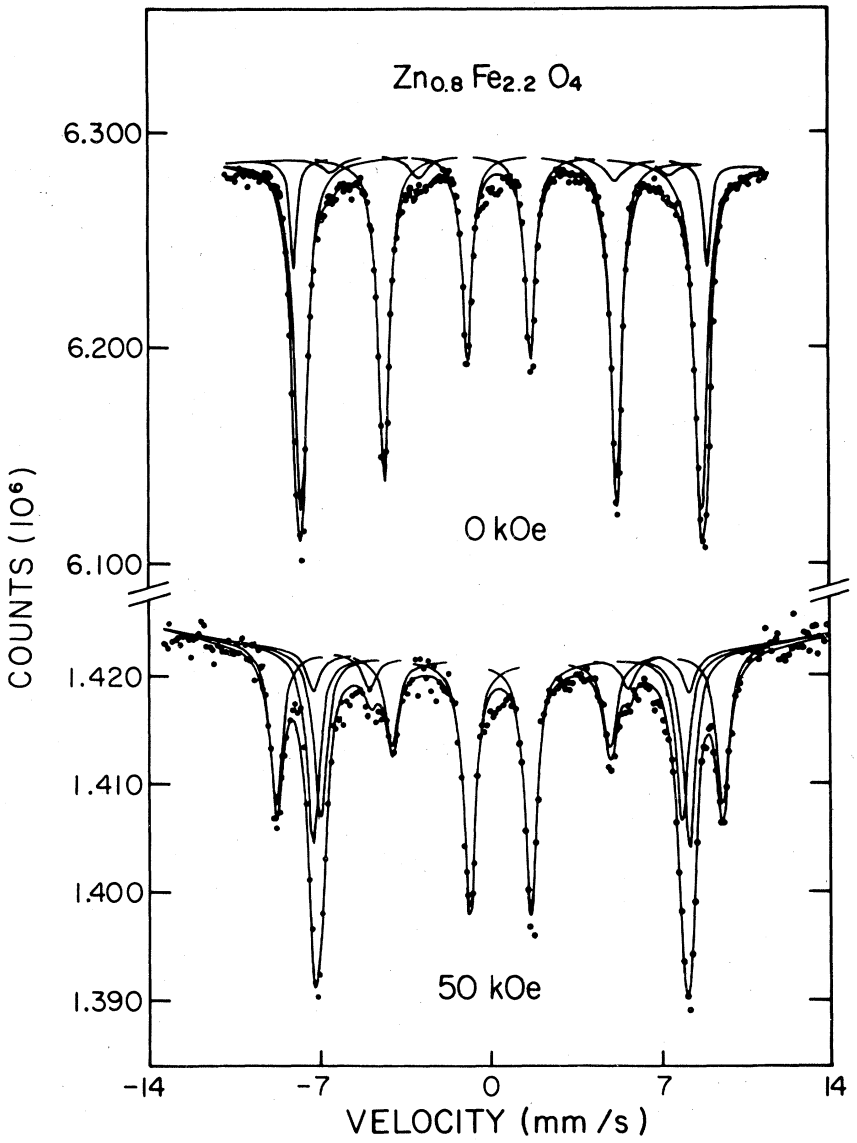

FIG. 10. Mössbauer spectra of $Zn_{0.8}Fe_{2.2}O_4$ at 4.2 K in applied fields of 0 and 50 kOe.

TABLE V. Experimental values of the isomer shifts δ (mm/s), hyperfine fields H_{hf} (kOe), and local canting angles ϕ (degrees) for Fe^{3+} ions in $Zn_xFe_{3-x}O_4$ at 4.2 K in various applied fields H_{ext} (kOe).

		A site		*B* site										
				B_{04}		B_5			$B_{6'}$			B_6		
x	H_{ext}	δ	H_{hf}	δ	H_{hf}	δ	H_{hf}	ϕ	δ	H_{hf}	ϕ	δ	H_{hf}
0.6	0	0.45(2)	511(10)	0.45(2)	511(10)	0.45(3)	511(10)		0.45(3)	511(10)			
	10	0.43(3)	521(5)	0.47(2)	505(5)	0.47(2)	505(5)	59(2)	0.43(3)	521(5)			
	25	0.34(9)	537(3)	0.48(3)	492(1)	0.48(3)	492(1)	40(2)	0.34(9)	537(3)			
	50	0.34(7)	561(2)	0.45(6)	463(1)	0.45(6)	463(2)	<20	0.45(6)	561(2)			
0.8	0	0.45(2)	508(10)	0.45(2)	508(10)	0.45(2)	508(10)		0.45(2)	508(10)		0.45(2)	508(10)
	8.6	0.30(2)	524(5)	0.32(2)	507(5)	0.32(2)	507(5)	65(12)	0.30(2)	524(5)		0.32(2)	507(5)
	15.4	0.40(2)	520(5)	0.49(1)	501(5)	0.49(2)	501(5)	60(2)	0.40(2)	520(5)		0.49(2)	501(5)
	30	0.47(3)	540(4)	0.47(3)	476(4)	0.49(9)	494(3)	54(5)	0.47(1)	540(4)	140(5)	0.47(1)	496(5)
	50	0.37(1)	566(3)	0.36(1)	460(1)	0.44(7)	478(1)	46(1)	0.37(1)	566(5)	142(1)	0.44(7)	477(1)

V. DISCUSSION

By using the canting angles determined from the Mössbauer study the magnetization can be calculated from Eq. (6) after values for the magnetic moments on the different sites have been assumed. By using free-ion magnetic moments of $\mu = 4\mu_B$ for Fe^{2+} and $\mu = 5\mu_B$ for Fe^{3+} ions, independent of the site occupied, the dependence of the magnetization on H_{ext} and x is in reasonable agreement with experiment.

In reality, the magnetic moments will be different from the free-ion values for the following two reasons: (i) The quenching of the orbital moment might not be complete, increasing the moment of the Fe^{2+} ions. (ii) Covalency effects could cause a change in the magnetic moments from the transfer of electrons into empty $3d$ orbitals, thus decreasing the magnetic moments for both Fe^{2+} and Fe^{3+}. Calculations have been made for Fe^{3+} ions on both A and B sites by Sawatzky and van der Woude; they find values of 4.31 and $4.62\mu_B$, respectively.[28] No values for Fe^{2+} ions are available.

The B-site Fe^{3+} hyperfine field at 0 K in spinels and garnets are typically close to 550 kOe.[29] As may be seen from Tables III, IV, and V, these hyperfine fields in $Zn_xFe_{3-x}O_4$ are ~510 kOe, independent of x, suggesting that covalency effects produce a magnetic moment ~10% smaller than the free-ion value. The Fe^{2+} hyperfine field at 4.2 K is dependent on x, which may be correlated to the change in covalency contributions caused by the expanding lattice (Fig. 2).

The saturation magnetization $M_s(x)$ at 4.2 K, obtained from Fig. 4 is plotted in reduced form, $\mu(x)/\mu(0)$, for several applied magnetic fields in Fig. 11. Also plotted are those values expected for free-ion magnetic moments with no canting angles. For the sample with $x = 0.2$ the deviation between the experimental and calculated result can in principle be modeled by assuming a canting angle of ~10°. However it is more likely that there is no canting in this sample since it has a high-field susceptibility which is essentially zero and for the $x = 0.4$ sample in 50 kOe no canting was observed, except possibly the 180° canting for the $B_{6'}$ component. For the $x = 0.2$ sample this component can be neglected.

By assuming a collinear spin system for the $x = 0.0$ and 0.2 samples, a Fe^{3+} moment on the B site of $\mu(Fe^{3+},B) = 4.55 \pm 0.06\mu_B$ and a difference between Fe^{3+} ion moments on A sites and Fe^{2+} ion moments on B sites of $0.35 \pm 0.01\mu_B$ are obtained for a fit of the $\mu(x)/\mu(0)$ values for $x = 0.0$ and 0.2 for fields $H_{ext} \geq 15$ kOe. The value of $\mu(Fe^{3+},B)$ agrees well with the value from the covalency calculation.[28] Subsequently the value of $\mu(Fe^{3+},A) = 4.31\mu_B$ was used from the same calculation; this then yields $\mu(Fe^{2+},B) = 4.0 \pm 0.1\mu_B$. The expected magnetization as a function of Zn substitution using these values and assuming no canting is also shown in Fig. 11 by the solid line.

For larger values of x ($x \gtrsim 0.4$), the experimental points deviated more and more from this theoretical fit. Further, the spread in $\mu(x)/\mu(x=0)$ for various applied fields increased with increasing Zn substitution. It will now be demonstrated that the localized canting of the spin structure found in this region can successfully account for these effects.

The sample $x = 0.4$ was analyzed at 0, 10, and 50 kOe. It was assumed that canting was uniform over the B site, although no B-site Fe^{2+} canting was allowed for in the fit because the 2–5 line intensity of

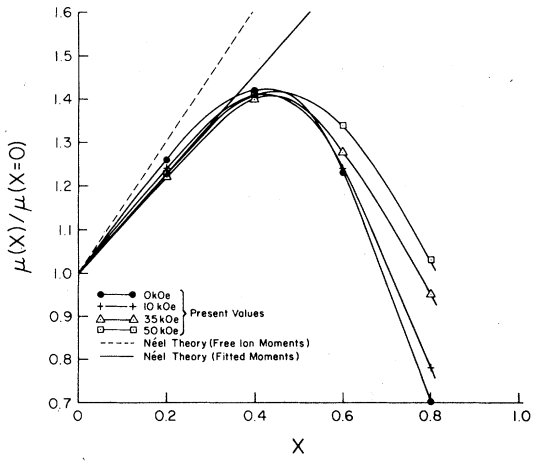

FIG. 11. Magnetic moment $\mu(x)$ per formula unit of $Zn_xFe_{3-x}O_4$ for various applied fields at 4.2 K. The dashed and full straight lines are based on theory; the full curves joining the experimental points are merely drawn as visual aids.

TABLE VI. Magnetic moment per chemical formula unit in Bohr magnetons, μ_B, for $Zn_xFe_{3-x}O_4$ as determined by magnetization measurements and as calculated from Mössbauer results.

x	H_{ext}	Magnetization Measured	Calculated
0.4	0	5.72(6)	...
	10	5.82(6)	5.6(3)
	50	6.07(6)	6.2(2)
0.6	0	4.99(5)	...
	10	5.16(5)	5.5(3)
	25	5.40(5)	6.0(3)
	25	5.78(6)	6.3(3)
0.8	0	2.84(3)	
	8.6	3.22(3)	3.2(3)
	15.4	3.54(4)	3.5(3)
	25	3.77(4)	3.8(2)
	50	4.47(5)	4.2(2)

that pattern was small. By using the values for the ionic moments calculated above and the formula

$$\mu(x=0.4, T=4.2\ \text{K}) = (1.4\mu_B^{3+} + 0.6\mu_B^{2+})\cos\bar{\theta}_B - 0.6\mu_\alpha$$

the moment for the bulk magnetization was calculated, and is compared to the experimental results in Table VI. These results clearly agree within the calculated errors.

The results obtained for the $x=0.6$ and 0.8 samples were analyzed for different fields, assuming that all canting occurs on B_5 and $B_{6'}$ sites. Magnetic moments per formula unit were calculated from Eq. (6). The measured and calculated magnetizations are also shown in Table VI. For the $x=0.6$ sample the theoretical values are an average of 10% higher than the measured magnetizations. No reasons for this discrepancy have been established. It can neither be accounted for in terms of absorber thickness effects nor in terms of an inaccuracy in the nominal Zn concentration. For the $x=0.8$ sample, clearly good agreement exists between the Mössbauer and magnetization measurements.

In conclusion, a magnetic structure is developed for $Zn_xFe_{3-x}O_4$ that is in good accord both with Mössbauer spectra and with magnetization data. This study supports the validity of the localized canting model provided it is generalized to include more structural details.

ACKNOWLEDGMENTS

We are grateful to Professor C. M. Srivastava of the Indian Institute of Technology, Bombay, India for providing the excellent quality samples. This research was made possible by grants from the National Science and Engineering Research Council of Canada.

---

*Now at: Allan Blair Memorial Clinic, Saskatchewan Cancer Foundation, Regina, SK, S4T 4L8 Canada.
†Now at: Coastal Marine Science Laboratory, Royal Roads Military College, FMO Victoria, BC, VOS 1B0 Canada.

[1]J. Smit and H. P. J. Wijn, *Ferrites* (Wiley, New York, 1959).
[2]U. König, E. F. Bertaut, Y. Gros, M. Mitrikov, and G. Chol, Solid State Commun. 8, 759 (1970).
[3]M. A. Gilleo, Phys. Chem. Solids 13, 33 (1960).
[4]I. Nowik, J. Appl. Phys. 40, 5184 (1969).
[5]Y. Ishikawa, J. Phys. Soc. Jpn. 17, 1877 (1962).
[6]V. C. Wilson and J. S. Kasper, Phys. Rev. 95, 1408 (1954).
[7]N. S. Satya Murthy, M. G. Natera, S. I. Youssef, R. J. Begum, and C. M. Srivastava, Phys. Rev. 181, 969 (1969).
[8]V. I. Goldanskii, V. F. Belov, M. N. Devisheva, and V. A. Irukhtanov, Zh. Eksp. Teor. Fiz. 49, 1681 (1965) [Sov. Phys. JETP 22, 1149 (1966)].
[9]J. M. Daniels and A. Rosencwaig, Can. J. Phys. 48, 381 (1970).
[10]L. K. Leung, B. J. Evans, and A. H. Morrish, Phys. Rev. B 8, 20 (1973).
[11]G. A. Petit, Solid State Commun. 13, 1611 (1973).
[12]P. E. Clark and A. H. Morrish, Phys. Status Solidi A 19, 687 (1973).
[13]A. H. Morrish and P. E. Clark, Phys. Rev. B 11, 278 (1975).
[14]A. H. Morrish and P. J. Schurer, Physica (Utrecht) 86 - 88B, 921 (1977).
[15]J. Piekoszevshi, L. Dabrowski, and J. Suwalski, Solid State Commun. 16, 75 (1975).
[16]A. L. Stuijts, D. Veeneman, and A. Broeses van Groenou, in *Ferrites, Proceedings of the International Conference,* edited by Y. Hoshino, S. Iida, and M. Sugimoto (University Park Press, Tokyo, 1971), p. 236.
[17]C. M. Srivastava, S. N. Shringi, R. G. Srivastava, and N. G. Nandikar, Phys. Rev. B 14, 2032 (1976).
[18]C. M. Srivastava, S. N. Shringi, and R. G. Srivastava, Phys. Rev. B 14, 2041 (1976).
[19]A. Rosencwaig, Can. J. Phys. 48, 2857 (1970).
[20]S. Geller, H. J. Williams, G. P. Espinosa, and R. C. Sherwood, Bell Sys. Tech. J. 43, 565 (1964).
[21]P. Dickof, M. Sc. thesis (University of Manitoba, 1977) (unpublished).
[22]J. Crangle and G. M. Goodman, Proc. R. Soc. London Ser. A 321, 477 (1971).
[23]*Mössbauer Effect Data Index Covering the 1974 Literature,* edited by J. G. Stevens and V. E. Stevens (Plenum, New York, 1975).
[24]T. F. Cranshaw, J. Phys. E 7, 497 (1974).
[25]S. Iida, K. Mizushima, M. Mizoguchi, J. Mada, S. Umemur, J. Yoshida, and K. Nakao, J. Phys. (Paris) 38, C1-73 (1977).
[26]R. S. Hargrove and W. Kündig, Solid State Commun. 8, 303 (1970).
[27]M. Rubinstein and D. W. Forester, Solid State Commun. 9, 1675 (1971).
[28]G. A. Sawatzky and F. van der Woude, J. Phys. (Paris) 35, C6-47 (1974).
[29]J. J. van Loef, Physica (Utrecht) 32, 2102 (1966).